

accepted by the PASP; December 7, 2004

## Carbon stars in the IRTS survey

T. Le Bertre

*LERMA, UMR 8112, Observatoire de Paris, 61 av. de l'Observatoire, F-75014 Paris,  
France*

`Thibaut.LeBertre@obspm.fr`

M. Tanaka<sup>1</sup>, I. Yamamura and H. Murakami

*Institute of Space and Astronautical Science, 3-1-1 Yoshinodai, Sagamihara, Kanagawa  
229-8510, Japan*

and

D.J. MacConnell

*Science Programs, Computer Sciences Corporation, Space Telescope Science Institute, 3700  
San Martin Drive, Baltimore, MD 21218, U.S.A.*

### ABSTRACT

We have identified 139 cool carbon stars in the near-infrared spectrophotometric survey of the InfraRed Telescope in Space (IRTS) from the conspicuous presence of molecular absorption bands at 1.8, 3.1 and 3.8  $\mu\text{m}$ . Among them 14 are new, bright ( $K \sim 4.0\text{--}7.0$ ), carbon stars. We find a trend relating the 3.1  $\mu\text{m}$  band strength to the  $K\text{--}L'$  color index, which is known to correlate with mass-loss rate. This could be an effect of a relation between the depth of the 3.1  $\mu\text{m}$  feature and the degree of development of the extended stellar atmosphere where dust starts to form.

*Subject headings:* – stars: carbon – stars: mass-loss – stars: AGB and post-AGB  
– infrared: stars

---

<sup>1</sup>National Astronomical Observatory, Mitaka, Tokyo, 181-8588, Japan

## 1. Introduction

Carbon stars have traditionally been searched for in optical surveys with objective-prism plates. They were selected either through, initially, C<sub>2</sub> bands in the blue (Secchi 1868) or, later, through CN bands in the “photographic infrared” (Nassau & Velghe 1964). More recently carbon stars have been selected from spectroscopic data obtained in the optical range in the course of the Sloan Digital Sky Survey (Margon et al. 2002).

Carbon stars have also been searched for in the IRAS survey on the basis of an emission feature visible at 11.3  $\mu\text{m}$  in the Low Resolution Spectra and attributed to silicon carbide (Volk & Cohen 1989; Epcstein et al. 1990). A method to find carbon stars undergoing mass loss by combining IRAS and near-infrared (1–5  $\mu\text{m}$ ) color indices has been proposed by Epcstein et al. (1987). This method has been successfully used by Guglielmo et al. (1993) to discover new infrared carbon stars.

Carbon stars have been found also by selecting candidates from near-infrared color indices and then performing optical spectroscopy (Mauron et al. 2004).

The formation processes of our Galaxy have left traces at large distances from the Sun which are best seen in the form of evolved stars. The fraction of carbon stars among evolved stars is an indicator of the metallicity in the original population, and there is evidence that this fraction is increasing with galactocentric distance (Guglielmo et al. 1993). Inventories of cool carbon stars are of special interest because as these objects are evolved they can be used to trace matter at large galactocentric distances out to the Magellanic Clouds (Ibata et al. 2001).

The latest published version of the General Catalog of Galactic Carbon Stars (CGCS) has 6891 entries (Alksnis et al. 2001); most of them have been found on objective-prism photographic plates.

In the present work, we examine the potential of finding carbon stars by using near-infrared spectro-photometric surveys. For that purpose we use the data provided by the Japanese space experiment IRTS.

## 2. Near-infrared spectro-photometry with the IRTS

The InfraRed Telescope in Space (IRTS) is a 15-cm diameter cooled telescope, operated in space, which surveyed, by continuous scanning,  $\sim 7\%$  of the sky (2700 deg.<sup>2</sup>) with 4 infrared instruments (Murakami et al. 1996). The Near-InfraRed Spectrometer (NIRS) is a grating spectrometer that covers two spectral ranges, 1.4–2.5  $\mu\text{m}$  and 2.8–4.0  $\mu\text{m}$ , with a

spectral resolution ranging from  $\sim 20$ , at short wavelengths, to  $\sim 40$  at the long wavelength end. The instrument was mainly designed to study the extended infrared emission and has an entrance aperture of  $8' \times 8'$ . However, more than 14 000 point sources were also detected as peaks (“events”) over this extended emission. Their spectra are useful to probe the physical properties of late-type stars (e.g. Matsuura et al. 1999). We have also exploited them to study the contribution of mass-losing AGB stars to the galactic cycle of matter (Le Bertre et al. 2001, Paper I, and 2003, Paper II).

Hereafter we use the 2002 data release (NIRS Point Source Catalogue –PSC– Version 1) which is described in Yamamura et al. (2003). For each event, a spectrum was constructed from the flux measurements in every channel by fitting the scan signal templates. Then the spectra corresponding to the same point source were identified and averaged. Errors are estimated from the errors on each measurement and the scatter of the data points<sup>1</sup>.

### 3. Cool carbon stars in the NIRS Point Source Catalogue

Cool carbon stars are known to show molecular absorption bands in the near-infrared range. A NIRS spectrum of a bright carbon star, Y Tau, is presented in Fig. 1. A  $C_2$  band at  $1.8 \mu\text{m}$ , a band attributed to  $C_2H_2$  at  $3.8 \mu\text{m}$  and a blend at  $3.1 \mu\text{m}$ , due to  $C_2H_2 + HCN$  (Ridgway et al. 1978), are clearly visible as well as the CO bands at  $1.6$  and  $2.3 \mu\text{m}$ . The  $C_2H_2$  band at  $3.8 \mu\text{m}$  may not be visible in all carbon stars: Yamamura et al. (1998) show that it is seen preferentially in the intermediate mass-losing stars of the class III defined by Groenewegen et al. (1992). Its presence may also depend on the phase of variability; for instance it is visible in all ISO Short Wavelength Spectrometer (SWS) spectra of V CrB except the one obtained close to maximum (see in Sect. 4.2, Fig. 9), possibly an effect of the strong dependence of the  $C_2H_2$  abundance on the stellar effective temperature (Matsuura et al. 2002). CN also contributes to the steep decline at the shortest wavelengths ( $\sim 1.4 \mu\text{m}$ ).

In general, the  $3.1 \mu\text{m}$  blend is much deeper than the band due to  $C_2$ . However, we caution that, in the NIRS spectra, the spectral resolution around  $1.8 \mu\text{m}$  is lower than around  $3.1 \mu\text{m}$  which may lead to underestimating the corresponding  $C_2$  band depth, the  $C_2$  band width being about  $0.05 \mu\text{m}$  (Lançon & Wood 2000). Also, as the entrance aperture was larger than the point sources, the individual spectra may have been displaced slightly over the detector array hindering the perception of this  $C_2$  band. This band can be useful when the signal-to-noise ratio is marginal in the range  $2.8$ – $4.0 \mu\text{m}$  (Fig. 2). Also it is reassuring

---

<sup>1</sup>The IRTS data and explanations are available via the DARTS archive; URL: <http://www.darts.isas.jaxa.jp/>.

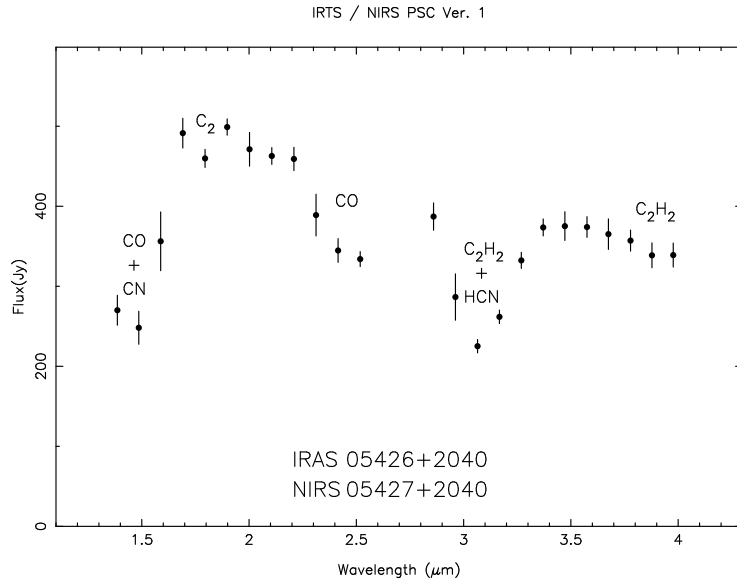


Fig. 1.— NIRS spectrum of CGCS 1042 ( $\equiv$  Y Tau; N2, C5II)

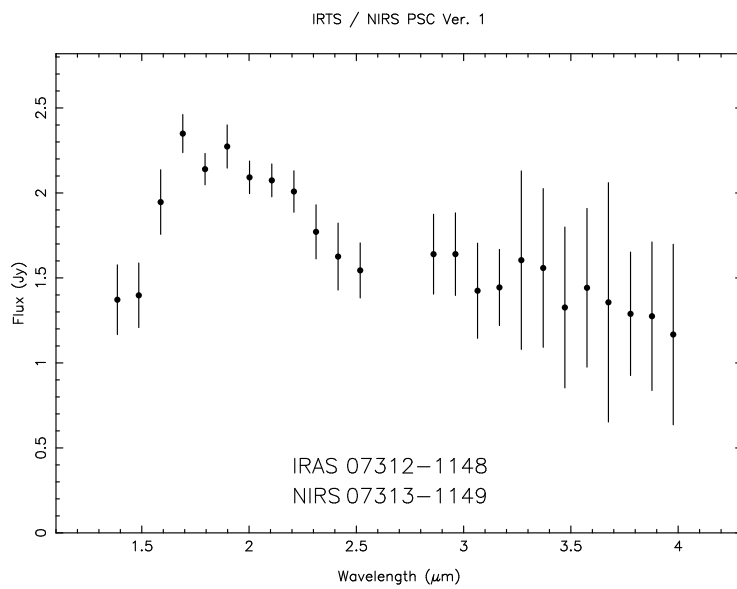


Fig. 2.— NIRS spectrum of CGCS 1767 (N).

to detect it as the presence of  $C_2$  absorption bands is the defining characteristic of C stars in the 0.4–0.6  $\mu\text{m}$  region.

The 3.1  $\mu\text{m}$  blend is seen even in highly reddened sources (Fig. 3) although it tends to be obliterated by circumstellar dust emission.

To identify carbon stars in the NIRS PSC, we use the 3.1  $\mu\text{m}$  index defined in Paper II. This index gives the depth of the band (at 3.1  $\mu\text{m}$ ) relative to the continuum (taken at 2.9 and 3.3  $\mu\text{m}$ ); the maximum depth is obtained for an index value of 0.0 whereas a value  $\sim 0.5$  indicates a flat spectrum. The strength of the 3.1  $\mu\text{m}$  feature has been found to be a very sensitive indicator of the C/O abundance ratio (Catchpole & Whitelock 1985).

In Paper II we have used this index to discriminate oxygen-rich stars from carbon-rich ones in a sample of 689 mass-losing AGB stars. A histogram of this sample is presented in Fig. 4. Most of the carbon stars have an index smaller than 0.45 (only 3 sources have an index larger than 0.45); the median value is at 0.34. On the other hand, the oxygen-rich stars have in general an index around 0.5.

We should note at this stage that there is, in principle, a difficulty with some S stars with a C/O abundance ratio close to 1, and in particular the SC stars. If such S/SC stars show the 3.1  $\mu\text{m}$  absorption band, with our procedure, they would be recognized as C stars, although strictly speaking they are only somewhat enriched in carbon. The SC class refers to stars that show ZrO bands and also CN bands. Some show the 3.1  $\mu\text{m}$  absorption band (Catchpole & Whitelock 1985) as well as a band attributed to CS around 4  $\mu\text{m}$  (Aoki et al. 1998). They constitute a rare group (only 14 SC stars are in the General Catalog of S Stars – Stephenson 1984) forming a continuous sequence from S to C stars. In principle, they do not show  $C_2$  bands (Stephenson 1984). As most of our sources show the  $C_2$  band at 1.8  $\mu\text{m}$  and as SC stars are rare, we do not expect a significant contamination. On the other hand, the discovery of more such rare objects would be of interest. In the IRTS survey, we found only one source (NIRS 19505+5332  $\equiv$  BS Cyg  $\equiv$  CGCS 4543) which belongs to this class. Its spectrum, for which only the odd-numbered channels were transmitted, shows clearly the absorption band at 3.1  $\mu\text{m}$  (Fig. 5). It is classified as SC8/8 by Keenan & Boeshaar (1980) but does not appear in Stephenson (1984). Catchpole & Whitelock (1985) note that the SC star BH Cru which has an absorption feature at 3.1  $\mu\text{m}$  may show occasionally characteristics of a CS star (Lloyd Evans 1985). This is supported by the recent discussion of this star by Zijlstra et al. (2004) who interpret such changes as a temperature effect.

Finally we note that some S stars show a weak absorption band at 3.1  $\mu\text{m}$ . Two such cases have been observed by ISO with the SWS: W Aql and S Cas. The near-infrared part of their spectra is shown in Fig. 6 together with the one of a carbon star, R Scl. The 3.1  $\mu\text{m}$

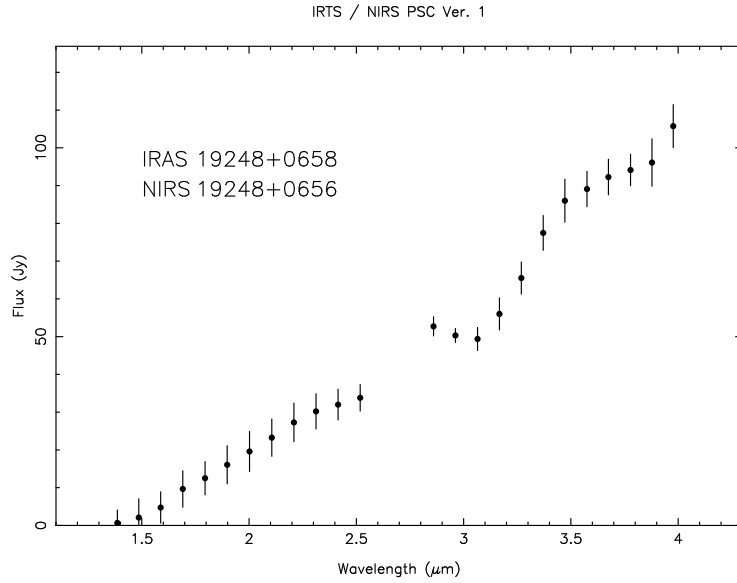


Fig. 3.— NIRS spectrum of CGCS 4275 ( $\equiv$  V1421 Aql, AFGL 2392).

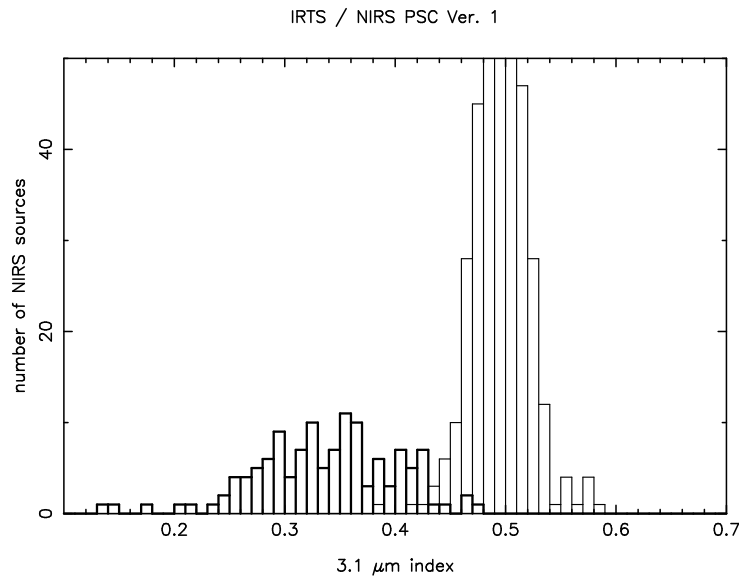


Fig. 4.— Histogram of the 3.1  $\mu\text{m}$  index for the sample of AGB mass-losing stars studied in Paper II. Thick line: 126 C-rich stars, thin line : 563 O-rich stars. For clarity the histogram has been truncated.

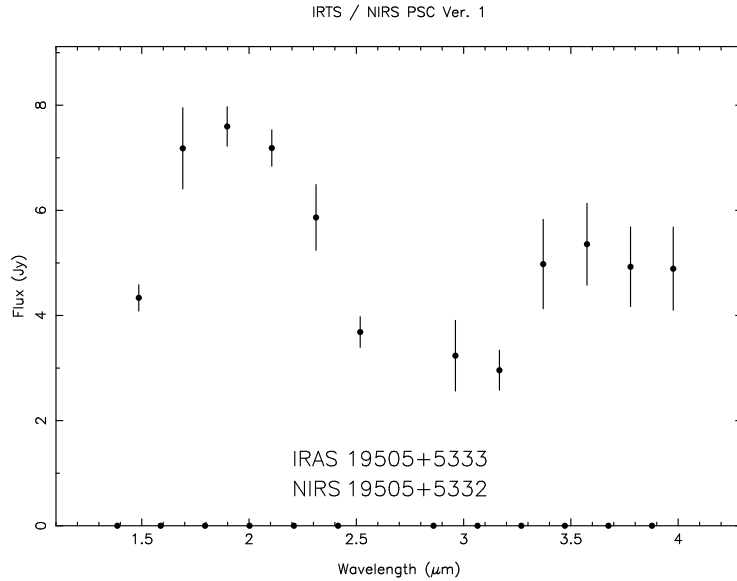


Fig. 5.— NIRS spectrum of BS Cyg ( $\equiv$  CGCS 4543; Nep, SC8/8).

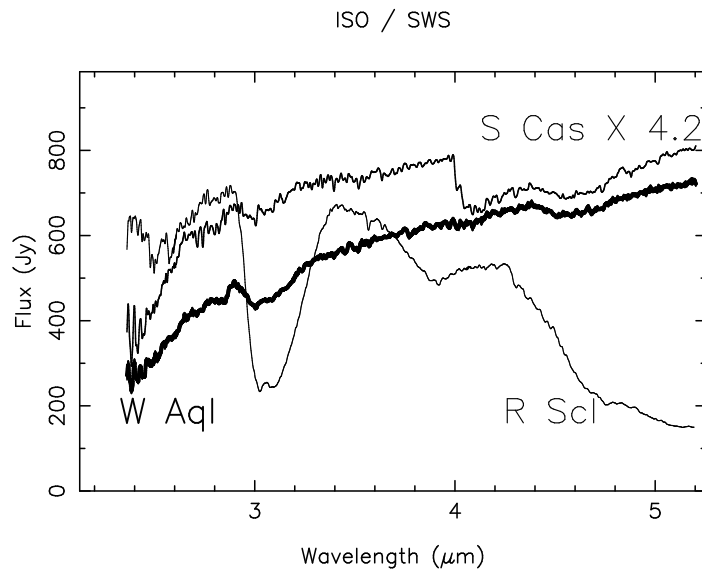


Fig. 6.— ISO/ SWS spectra of two S-type stars, W Aql (CSS 1115, thick line) and S Cas (CSS 28, medium line), and one C-type star, R Scl (CGCS 234, thin line). A factor of 4.2 has been applied to the spectrum of S Cas.

blend is visible clearly in R Scl and W Aql and seems also present in S Cas. The latter source has been observed by the IRTS, but the  $3.1\text{ }\mu\text{m}$  band is not visible in the NIRS spectrum (see Fig. 4 in Paper I). The source W Aql is not in the NIRS PSC; the  $3.1\text{ }\mu\text{m}$  index measured on the ISO spectrum is  $\sim 0.46$ . On the other hand, the  $\text{C}_2\text{H}_2$  band at  $3.8\text{ }\mu\text{m}$  is present in the spectrum of R Scl but not in the spectra of the two S stars. There is an absorption from  $4.0$  to  $4.2\text{ }\mu\text{m}$  due to SiO in the spectrum of S Cas and perhaps W Aql but not in the one of R Scl. At the present stage, we conclude that some S-type stars may show the  $3.1\text{ }\mu\text{m}$  absorption band, and we suspect that they do not show the band of  $\text{C}_2\text{H}_2$  at  $3.8\text{ }\mu\text{m}$ . For these stars, the  $3.1\text{ }\mu\text{m}$  seems to stay weak, and we expect that a limit of 0.45 on the index value keeps them out of our selection.

We have considered the 8879 NIRS sources for which the data are of sufficiently good quality to estimate their K and L' magnitudes in the ESO photometric system (see Paper II). Among them we obtained 471 sources with a  $3.1\text{ }\mu\text{m}$  index  $\leq 0.45$ . Each corresponding spectrum was examined visually. We found 139 sources that unambiguously show a  $\text{C}_2$  band at  $1.8\text{ }\mu\text{m}$  and/or the blend at  $3.1\text{ }\mu\text{m}$  and 220 which are very probably not carbon-rich. The former are reported in Table 2. Most of these carbon stars can be associated with an IRAS and a CGCS source. However, these associations should be viewed with caution because the entrance aperture of the NIRS on the sky was  $8'\times 8'$ . Also, the accuracy of the pointing reconstruction is  $\sim 2'$  r.m.s.

Some carbon stars may have been missed, for instance among the remaining 112 sources for which the NIRS spectra do not have a signal-to-noise ratio sufficient to characterize them. Also, we remind that some carbon stars may have a  $3.1\text{ }\mu\text{m}$  index above 0.45: three such cases were identified in Paper II (see also Fig. 4). For clarity, we have added these 3 cases at the end of Table 2. The majority of the 220 sources that we have rejected have a  $3.1\text{ }\mu\text{m}$  index in the range 0.40–0.45. Also, there are sources which show an emission band at  $3.3\text{ }\mu\text{m}$  attributed to PAHs. This emission raises the flux at  $3.3\text{ }\mu\text{m}$  relative to  $3.1\text{ }\mu\text{m}$  which mimics an absorption. These “PAH” sources, which often have a large K–L', are readily identified from their NIRS spectra. Finally, it is worth noting that we did not find carbon stars with a K–L' color smaller than 0.4.

Tanaka et al. (in preparation) have developed a similar, but slightly different, method. They use 5 parameters to separate M, C and S stars. Applying this method to 4002 NIRS spectra of good quality, they find 91 carbon stars. With our procedure we have obtained all their carbon stars, but one (NIRS 07281–1216  $\equiv$  IRAS 07280–1217  $\equiv$  CGCS 1735). This source shows a weak  $3.1\text{ }\mu\text{m}$  absorption band ( $3.1\text{ }\mu\text{m}$  index = 0.46) which explains why we could not select it. For completeness we have added this source at the end of Table 2. The incidence of carbon stars in their sample is about 0.023 (91/4002), whereas it is about 0.016

(139/8879) in our sample. This confirms that we miss some carbon stars at low signal-to-noise ratio.

The few sources (14) in Table 2 that have no CGCS counterpart can be considered as new cool carbon stars. Their NIRS spectra are given in Fig. 11. It is surprising that new carbon stars are found that do not have an extreme color ( $K-L' \leq 1$ ) and still are relatively bright ( $K \sim 6$ ). Perhaps they have been missed in previous surveys because they are variable. Some of these new carbon stars are in fields covered by near-IR objective-prism plates obtained by one of us (MacConnell 2003). These plates have been re-examined, and the results are given in the notes to Table 2.

## 4. Discussion

### 4.1. Cool carbon stars

In the upper panel of Fig. 7 we present the  $3.1 \mu\text{m}$  index as a function of  $K-L'$ . Most of the 8879 NIRS sources with available  $K$  and  $L'$  magnitudes are in a large clump around an index value of  $\sim 0.50$  and a  $K-L'$  color of  $\sim 0.3$ . There is a tail going horizontally to the right and composed mainly of oxygen-rich late-type stars. In addition, there is a “plume” going downward to the right, which is marked by a straight line in the figure. This plume is made of carbon stars as can be seen in the lower panel of the figure.

This feature shows that there is a relation between the  $3.1 \mu\text{m}$  index that characterizes the carbon-rich stellar atmospheres and the  $K-L'$  color in the range 0.7 to 1.4. This color is known to be related to the present mass-loss rate of carbon stars (Le Bertre 1997). It is interesting to note that the same kind of plume is visible when plotting the  $1.9 \mu\text{m}$  index (which characterizes O-rich late-type stars) versus  $K-L'$  which, for these sources, characterizes their present mass-loss rate (Le Bertre & Winters 1998). The trend is not a perfect correlation and sources are found also to the right of the plume. This might be an effect of dust emission filling in the  $3.1 \mu\text{m}$  band in spectra of sources undergoing heavy mass loss. Groenewegen et al. (1994) have obtained  $2.8$ – $3.5 \mu\text{m}$  spectra for 16 carbon stars with a  $K-L$  index in the range 2–7. They find that the  $3.1 \mu\text{m}$  feature weakens with redder  $K-L$  color and interpret this tendency also as an effect of filling-in by dust emission.

A possible interpretation of the trend observed in Fig. 7 is that the mass loss and the absorption band at  $3.1 \mu\text{m}$  are both increasing with the degree of development of the extended stellar atmosphere where dust is likely to form. Winters et al. (2000) have shown that the mass loss of red giants is favored by a low effective temperature, a low stellar mass, a high luminosity and a large pulsation amplitude. The synthetic spectra of carbon-rich AGB star

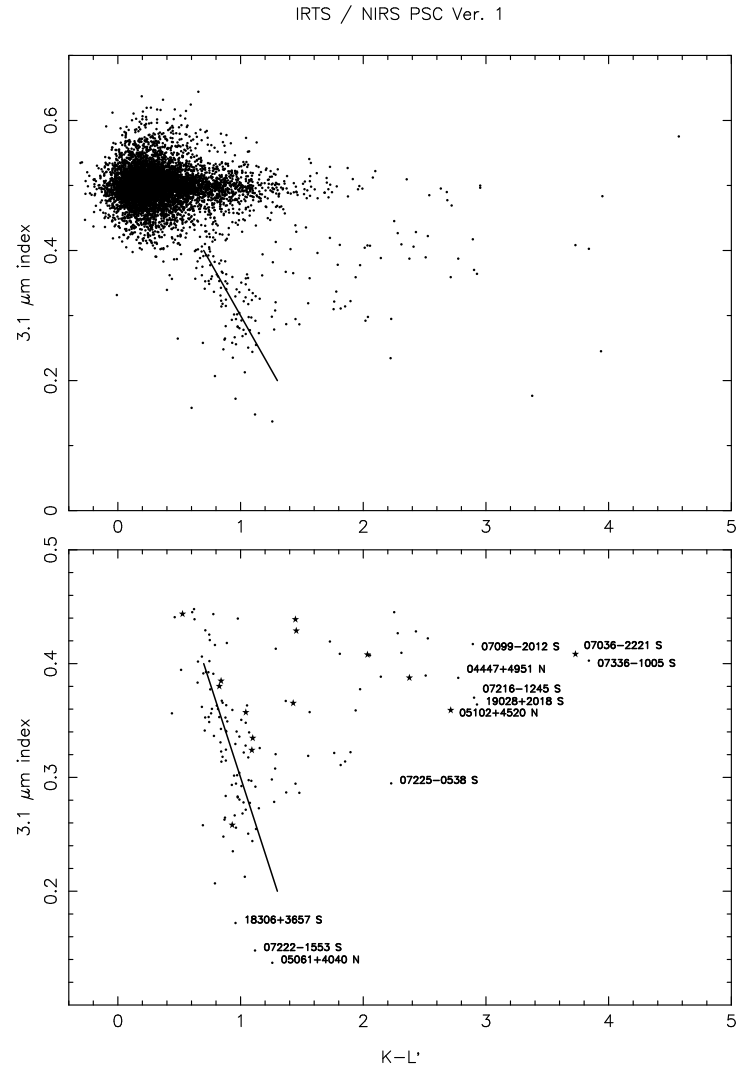


Fig. 7.—  $3.1 \mu\text{m}$  index versus  $\text{K}-\text{L}'$ . Upper panel: All NIRS sources (8879). Lower panel: carbon-rich sources (139); the most extreme sources are marked by their NIRS identifiers and the 14 new carbon stars are represented by a  $\star$ .

atmospheres obtained by Loidl et al. (1999) from dynamic models show that the strengths of the  $C_2H_2$  and HCN features increase in the same manner, because these molecules form preferentially at low temperature ( $T < 2500$  K) in the upper atmospheric layers.

We have found 14 new carbon stars in a sample of 139 sources. The  $C_2$  band at 1.8  $\mu m$  has been useful to confirm the carbon-rich nature of the sources in the cases for which the signal-to-noise ratio at 3  $\mu m$  is poor. Unfortunately, the spectral resolution of the NIRS around 2  $\mu m$  ( $\sim 20$ ) is not enough to define an index measuring the depth of this band.

The IRTS survey is limited in sensitivity to  $K \sim 8$  and  $L' \sim 7$ ; furthermore in some regions of the sky, close to the Galactic Plane where the level of the extended emission is increased by confusion, the sensitivity was reduced by  $\sim 2$  magnitudes (Paper II). Most of the carbon stars that we have identified are probably at a distance between 1 and 5 kpc from the Sun (see Figure 7 in Paper II). Extrapolating to the whole sky, a survey like the IRTS would reveal  $\sim 2000$  cool carbon stars with possibly 200 new ones. These estimates would rise greatly for a survey with better sensitivity, spatial resolution and spectral resolution.

The advantages of searching for cool carbon stars by near-infrared spectro-photometric means are multiple. The effective temperature of N-type stars ranges from 1800 to 4000 K (Bergeat et al. 2001), and they reach the maximum of their energy distribution around 2  $\mu m$ . Many of them are undergoing mass loss and are surrounded by circumstellar dust shells which shift their spectra towards long wavelengths ( $\sim 3 \mu m$  or more). As a result of the energy distribution, the infrared data provides also a more direct determination of the luminosity than those obtained in the optical. Furthermore, carbon stars are often variable with an amplitude which decreases with wavelength; therefore, it is less likely to miss a star that is at minimum if the survey is done at a long wavelength. There is also a general advantage of the infrared range for detecting sources in regions of the Galaxy which are affected by dust extinction (“zone of avoidance”). Finally, as cool carbon-star spectra are characterized by wide molecular bands, a spectral resolution of  $\geq 40$  is enough to clearly recognize them. With spectro-photometry it is easy to build photometric indices targeted to specific classes of sources. On the other hand, our experience (Sect. 3) shows that the availability of a continuous spectrum over a large wavelength range is useful to identify the sources that contaminate the samples which are extracted on the basis of these photometric indices: the same data are used to select candidates and to confirm them.

#### 4.2. Other carbon stars in the IRTS survey

There are other categories of carbon stars, the majority being found in the R and CH classes. The R stars are a mix of giants with effective temperature lower than  $\sim 5000$  K, in general non-variable, and of classical cool carbon stars (late R type/ N type). The R stars proper (excluding N type) are too faint to be on the AGB and do not show evidence of mass loss. They may owe their carbon enrichment to an He-core flash (Dominy 1984) and, perhaps, to a coalescence in a binary system (McClure 1997). They are more easily selected by isolating the early R0–R4 sub-types.

A search for R stars in the NIRS PSC was performed by cross-correlating the positions in the PSC with those in the CGCS catalogue (Alksnis et al. 2001). We found several associations. The NIRS spectra of sources associated with early (R0–R4) type stars show sometimes CO absorptions at 1.6 and 2.3  $\mu\text{m}$ , but no other distinctive features (Fig. 8, upper panel). R stars of later type may show the C<sub>2</sub> band at 1.8  $\mu\text{m}$  without the 3.1  $\mu\text{m}$  absorption band (Fig. 8, lower panel), confirming our suspicion that the latter is not sufficient to select all cool carbon stars. It thus appears again that the 1.8  $\mu\text{m}$  band, as well as the 3.1  $\mu\text{m}$  band, could be very useful for future surveys.

The galactic CH stars are metal-poor carbon stars which are characterized in the optical range by strong CH bands. They are spectroscopic binaries and probably owe their carbon enrichment to mass transfer from a more evolved companion (Jorissen 1999). We have not identified any CH star in the NIRS PSC. However, at least 3 members of this class (V Ari, V CrB, HD 189711) were observed by ISO with the SWS. Apart from the long wavelength wing of the 2.3  $\mu\text{m}$  CO band, no characteristic feature is visible in the (2.3–4.1  $\mu\text{m}$ ) spectra of V Ari and HD 189711; unfortunately, the region of the spectrum around 1.8  $\mu\text{m}$  is missing in the ISO spectra. V CrB shows a strong absorption at 3.1  $\mu\text{m}$  and at some phases an absorption at 3.8  $\mu\text{m}$  (Fig. 9). However, this source is a Mira variable and therefore probably not typical of the CH class. If objects like V CrB are in the NIRS PSC, they would be selected as cool carbon stars and probably not recognized as being of the CH-type.

There are also the J-type stars which are characterized by strong <sup>13</sup>C bands indicating a low ( $\leq 10$ ) <sup>12</sup>C/<sup>13</sup>C ratio. We have identified three such cases which were already selected in Sect. 3: NIRS 07235–0354 (CGCS 1708), NIRS 12545+6615 (CGCS 3313, RY Dra) and NIRS 18306+3657 (CGCS 4038, T Lyr). All show strong molecular bands at 1.8 and 3.1  $\mu\text{m}$ . At the low spectral resolution of the NIRS, it does not seem possible to isolate the J-type stars from the other cool carbon stars.

We found 3 NIRS sources which could be associated with RV Tauri stars (Table 1).

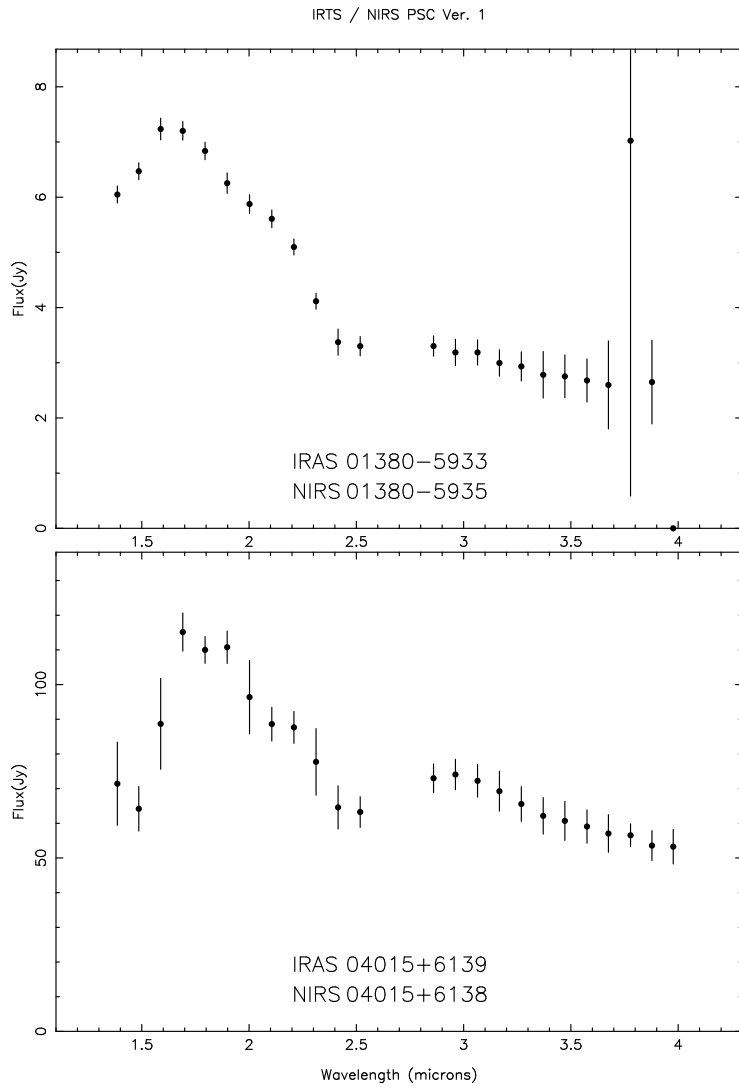


Fig. 8.— NIRS spectra of two R-type stars. Upper panel: CGCS 77 (R3). Lower panel: CGCS 177 (UV Cam, R8).

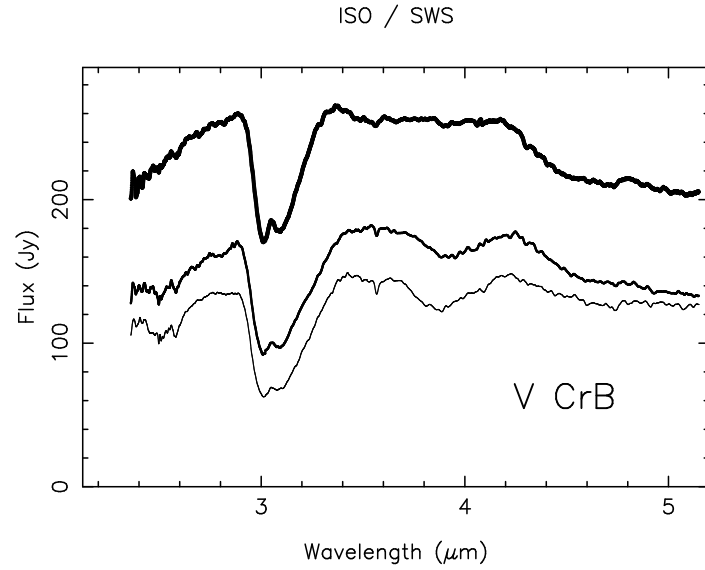


Fig. 9.— ISO SWS spectra of a CH star (V CrB, CGCS 3652) obtained at 3 different phases. Note that the  $3.8\ \mu\text{m}$  absorption is virtually absent (as well as the  $3.56\ \mu\text{m}$  HCN band) close to maximum (thick line), but clearly present close to minimum (medium and thin lines).

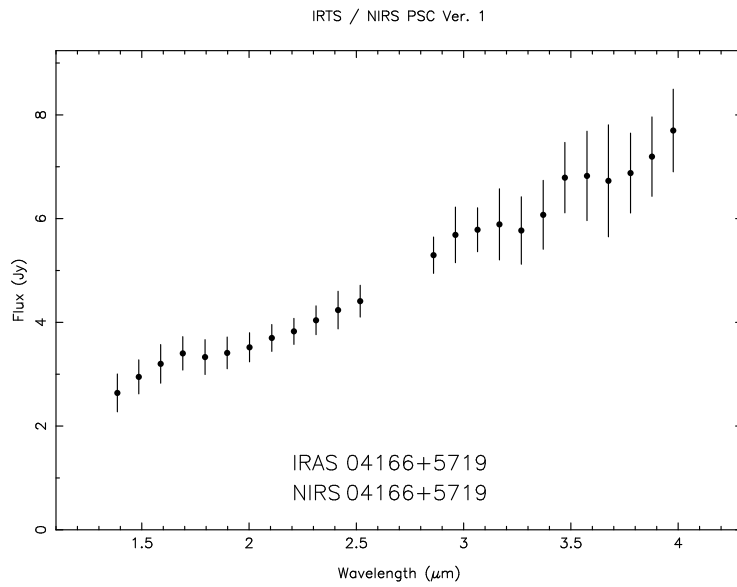


Fig. 10.— NIRS spectrum of TW Cam, a carbon-rich RV Tauri star (RVa; F8Ib).

It is known that some RV Tauri show a carbon-rich nature. Giridhar et al. (2000) have performed an abundance analysis of several RV Tauri stars: U Mon is O-rich ( $C/O \sim 0.8$ ) whereas TW Cam is carbon-rich ( $C/O \sim 2$ ). The O-rich character of U Mon is supported by its IRAS Low Resolution Spectrum (LRS class 26). Le Bertre et al. (2001) note that, in a  $K-L'$  versus  $12-25\mu m$  diagram, TW Cam falls in the 'c' (carbon-rich) region of Epchtein et al. (1987). The NIRS spectra corresponding to TW Cam (Fig. 10) and U Mon are basically featureless, whereas the one of NIRS 18125+0510 shows an  $H_2O$  band at  $1.9\mu m$  and a CO band at  $2.3\mu m$ . The latter NIRS source is certainly not carbon-rich.

Finally we could not identify RCB stars in the NIRS PSC, nor any known carbon-rich post-AGB stars. At the present stage, we do not see an easy way to pinpoint warm carbon stars directly in the IRTS survey.

## 5. Conclusion

We have identified 139 cool carbon stars in the IRTS/NIRS survey on the basis of the  $3.1\mu m$  absorption feature due to a blend of  $C_2H_2$  and HCN bands. About 90% have been confirmed through cross-identification with the CGCS and 14 are new, relatively bright ( $K \sim 3.9-6.9$ ), C stars. This indicates that an important number of bright carbon stars are still missing from our inventories.

It is likely that there are more cool carbon stars in the Point Source Catalogue that were not selected either because the  $3.1\mu m$  band is weak or because a limited signal-to-noise ratio hampered an unambiguous classification. The spectral resolution of the IRTS was insufficient to fully exploit the important  $C_2$  band at  $1.8\mu m$ ; a spectral resolution of 40 or better would have been preferable. The  $C_2$  band at  $1.8\mu m$  and the  $C_2H_2$  band at  $3.8\mu m$  should be useful to separate C from S stars. An extension of the wavelength coverage beyond  $4\mu m$  to cover the  $SiO$  band would also have been helpful.

Sensitive near-infrared spectro-photometric surveys covering the range from  $\sim 1.5$  to  $\sim 4.5\mu m$  with a spectral resolution  $\geq 40$  have therefore the potential to reveal new carbon

Table 1: Other candidate stars.

NIRS name	K	$K-L'$	IRAS association	other ass.	Spec. type	reference
04166+5719 N	5.57	1.70	04166+5719	TW Cam	F8Ib	Simbad
07284-0940 S	3.61	1.33	07284-0940	U Mon	K0Ibpvar	Simbad
18125+0510 N	5.19	1.07	18123+0511		G5	Mass (2003)

stars in the Galaxy and in its satellites, as well as in other galaxies, and to provide useful information on their physical properties.

We thank Dr. N. Epcstein for useful advice and encouragement. This research has made use of the SIMBAD database, operated at CDS, Strasbourg, France. We thank an anonymous referee for helpful suggestions.

Facilities: IRTS(NIRS), ISO(SWS).

## REFERENCES

Alksnis, A., Balklavs, A., Dzervitis, U., Eglitis, I., Paupers, O., & Pundure, I. 2001, Baltic Astron. 10, 1

Aoki, W., Tsuji, T., & Ohnaka, K. 1998, A&A 340, 222

Bergeat, J., Knapik, A., & Rutily, B. 2001, A&A 369, 178

Catchpole, R.M., & Whitelock, P.A. 1985, “Cool Stars with Excesses of Heavy Elements”, M. Jaschek and P.C. Keenan (eds), Dordrecht, D. Reidel Publishing Company, p19

Chen, P.-S., & Chen, W.-P. 2003, AJ 125, 2215

Dominy, J.F. 1984, ApJS 55, 27

Epcstein, N., Le Bertre, T., Lépine, J.R.D., Marques Dos Santos, P., Matsuura, O.T., & Picazzio, E. 1987, A&AS 71, 39

Epcstein, N., Le Bertre, T., & Lépine, J.R.D. 1990, A&A 227, 82

Giridhar, S., Lambert, D.L., & Gonzalez, G. 2000, ApJ 531, 521

Groenewegen, M.A.T., de Jong, T., van der Bliek, N.S., Slijkhuis, S., & Willems, F.J. 1992, A&A 253, 150

Groenewegen, M.A.T., de Jong, T., & Geballe, T.R. 1994, A&A 287, 163

Guglielmo, F., Epcstein, N., Le Bertre, T., Fouqué, P., Hron, J., Kerschbaum, F., & Lépine, J.R.D. 1993, A&AS 99, 31

Ibata, R., Irwin, M., Lewis, G.F., & Stolte, A. 2001, ApJ 547, L133

Jorissen, A. 1999, IAU S191, 437

Keenan, P.C., & Boeshaar, P.C. 1980, *ApJS* 43, 379

Kwok, S., Volk, K., & Bidelman, W.P. 1997, *ApJS* 112, 557

Lançon, A., & Wood, P.R. 2000, *A&AS* 146, 217

Le Bertre, T. 1997, *A&A* 324, 1059

Le Bertre, T., Matsuura, M., Winters, J.M., Murakami, H., Yamamura, I., Freund, M., & Tanaka, M. 2001, *A&A* 376, 997 (Paper I)

Le Bertre, T., Tanaka, M., Yamamura, I., & Murakami, H. 2003, *A&A*, 403, 943 (Paper II)

Le Bertre, T., & Winters, J.M. 1998, *A&A* 334, 173

Lloyd Evans, T. 1985, “Cool Stars with Excesses of Heavy Elements”, M. Jaschek and P.C. Keenan (eds), Dordrecht, D. Reidel Publishing Company, p163

Loidl, R., Höfner, S., Jørgensen, U.G., & Aringer, B. 1999, *A&A* 342, 531

MacConnell, D.J. 1979, *A&AS* 38, 335

MacConnell, D.J. 2003, *PASP* 115, 351

Margon, B., Anderson, S.F., Harris, H.C., et al. 2002, *AJ* 124, 1651

Mass, T. 2003, PhD thesis, University of Leuven

Matsuura, M., Yamamura, I., Murakami, H., Freund, M.M., & Tanaka, M. 1999, *A&A* 348, 579

Matsuura, M., Zijlstra, A.A., van Loon, J.T., Yamamura, I., Markwick, A.J., Woods, P.M., & Waters, L.B.F.M. 2002, *ApJ* 530, L133

Mauron, N., Azzopardi, M., Gigoyan, K., & Kendall, T.R. 2004, *A&A* 418, 77

McClure, R.D. 1997, *PASP* 109, 256

Murakami, H., Freund, M.M., Ganga, K., et al. 1996, *PASJ* 48, L41

Nassau, J.J., & Velghe, A.G. 1964, *ApJ* 139, 190

Ridgway, S.T., Carbon, D.F., & Hall, D.N.B. 1978, *ApJ* 225, 138

Secchi, A. 1868, *Comptes Rendus Acad. Sc. Paris* 66, 124

Stephenson, C.B. 1984, *Publ. Warner & Swasey Obs.*, 3, 1

Volk, K., & Cohen, M. 1989, *AJ* 98, 931

Winters, J.M., Le Bertre, T., Jeong, K.S., Helling, Ch., & Sedlmayr, E. 2000, *A&A* 361, 641

Yamamura, I., de Jong, T., Justtanont, K., Cami, J., & Waters, L.B.F.M. 1998, *Ap&SS* 255, 351

Yamamura, I., Tanaka, M., Takahashi, H., et al. 2003, Exploiting the ISO Data Archive – Infrared Astronomy in the Internet Age, C. Gry et al. (eds), *ESA–SP* 511, p. 35

Zijlstra, A.A., Bedding, T.R., Markwick, A.J., et al. 2004, *MNRAS* 352, 325

### A. Appendix material

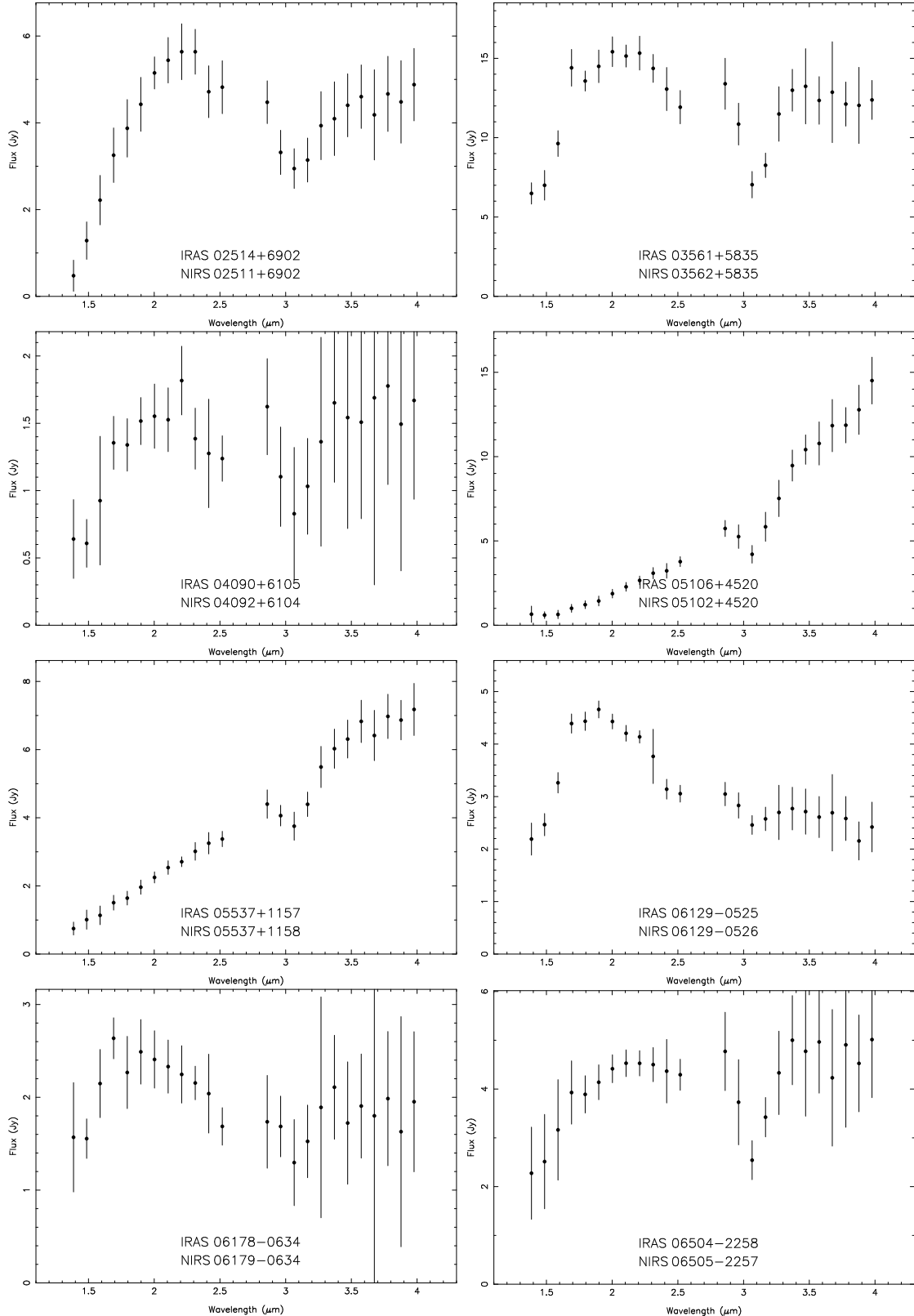


Fig. 11.— NIRS spectra of new carbon stars.

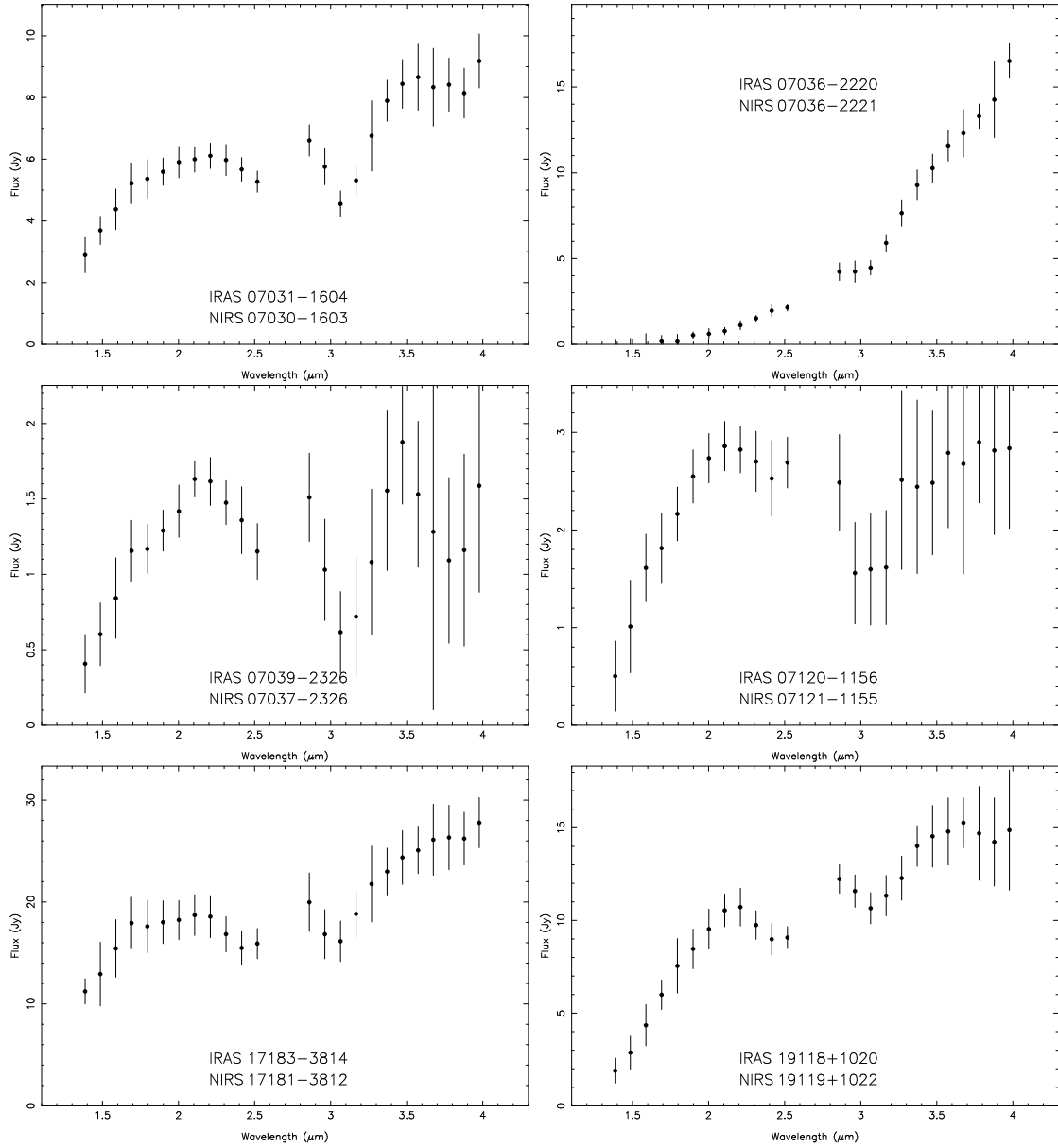


Fig. 11.— NIRS spectra of new carbon stars (continued).

Table 2. IRTS carbon-stars.

NIRS name	$l^{\text{II}}$	$b^{\text{II}}$	K	$K-L'$	$3.1 \mu\text{m}$	IRAS	CGCS	comments
00593+7135 N	123.83	9.01	4.77	0.69	0.41	00591+7133	CGCS	163
01414+7104 N	127.27	8.91	4.14	1.37	0.29	01411+7104	CGCS	261
02511+6902 N	133.60	8.98	5.18	0.84	0.38	02514+6902		
02596+6638 N	135.45	7.25	4.56	2.28	0.43	02596+6639	CGCS	430
03063+6552 N	136.43	6.91	5.83	1.03	0.21	03063+6553	CGCS	6044
03171+6515 N	137.71	6.98	4.71	0.75	0.43	03170+6515	CGCS	6050
03285+6318 N	139.83	6.03	6.78	1.01	0.35		CGCS	509
03375+6229 N	141.15	5.98	0.48	0.84	0.33	03374+6229	CGCS	540
03562+5835 N	145.40	4.37	4.10	0.84	0.31	03561+5835	CGCS	583
03562+5911 N	145.01	4.82	6.11	2.38	0.39	03561+5912		
03576+5923 N	145.02	5.10	4.23	1.45	0.29	03575+5922	CGCS	591
04035+5929 N	145.51	5.66	5.15	1.29	0.41	04035+5929	CGCS	613
04092+6104 N	144.95	7.30	6.56	1.09	0.32	04090+6105		
04165+5703 N	148.44	5.06	5.36	0.88	0.34	04164+5701	CGCS	656
04207+5549 N	149.72	4.59	4.13	1.04	0.33	04207+5548	CGCS	674
04217+5401 N	151.11	3.43	5.59	1.08	0.28	04216+5401	CGCS	677
04296+5253 N	152.75	3.50	5.28	0.79	0.42	04295+5252	CGCS	713
04354+5414 N	152.33	5.04	5.00	0.96	0.26	04354+5415	CGCS	730
04393+4905 N	156.59	2.07	5.76	2.14	0.39	04391+4904	CGCS	6085
04426+4950 N	156.37	2.97	4.68	1.56	0.36	04427+4951	CGCS	763
04447+4951 N	156.58	3.24	4.66	2.77	0.39	04449+4951	CGCS	772
04468+4930 N	157.07	3.27	5.14	0.94	0.24	04468+4930	CGCS	784
04500+4802 N	158.54	2.74	5.38	1.28	0.31	04500+4802	CGCS	801
04504+4950 N	157.19	3.94	2.85	1.12	0.29	04504+4949	CGCS	806
04540+4450 N	161.45	1.24	6.11	0.87	0.26	04539+4450	CGCS	817
04553+4925 N	158.02	4.28	5.35	0.88	0.34	04552+4925	CGCS	820
05058+3855 N	167.47	-0.65	2.39	0.71	0.43	05056+3856	CGCS	860
05061+3956 N	166.69	0.00	5.11	1.82	0.31	05061+3956	CGCS	862
05061+4040 N	166.11	0.45	5.72	1.26	0.14	05062+4040	CGCS	863
05068+3945 N	166.92	0.00	4.27	0.96	0.29	05068+3945	CGCS	867
05102+4520 N	162.81	3.82	5.98	2.71	0.36	05106+4520		
05151+3511 N	171.57	-1.36	3.61	1.97	0.38	05149+3511	CGCS	900
05158+3545 N	171.20	-0.92	2.72	0.65	0.38	05158+3544	CGCS	904
05209+3430 N	172.81	-0.78	5.58	1.13	0.25	05209+3430	CGCS	921
05213+4001 N	168.32	2.42	4.25	1.48	0.29	05214+4001	CGCS	924
05237+3405 N	173.49	-0.54	1.50	1.55	0.32	05238+3406	CGCS	941
05276+3437 N	173.50	0.43	4.80	1.04	0.35	05278+3437	CGCS	961
05278+3151 N	175.82	-1.06	4.41	0.88	0.35	05278+3152	CGCS	962
05285+2814 N	178.92	-2.94	5.06	0.75	0.38	05285+2814	CGCS	964
05287+2930 N	177.90	-2.20	4.67	0.85	0.37	05288+2929	CGCS	966
05292+2938 N	177.84	-2.03	3.89	0.97	0.34	05292+2938	CGCS	971
05334+3057 N	177.23	-0.56	5.24	1.81	0.41	05334+3057	CGCS	999
05346+3001 N	178.16	-0.84	3.36	1.03	0.32	05345+3002	CGCS	1003
05352+2247 N	184.34	-4.64	3.10	0.96	0.33	05352+2247	CGCS	1006
05370+2629 N	181.43	-2.29	5.76	1.29	0.32	05371+2630	CGCS	1012
05416-4628 S	252.94	-30.71	1.13	0.95	0.27	05418-4628	CGCS	1052

Table 2—Continued

NIRS name	$l^{\text{II}}$	$b^{\text{II}}$	K	$K-L'$	$3.1 \mu\text{m}$	IRAS	CGCS	comments
05427+2040 N	187.07	−4.26	0.44	0.83	0.35	05426+2040	CGCS 1042	Fig. 1
05465+1440 N	192.70	−6.59	4.63	1.16	0.33	05464+1440	CGCS 1076	
05537+1158 N	195.93	−6.41	5.94	2.03	0.41	05537+1157		
05555+1235 N	195.62	−5.74	4.57	1.07	0.30	05557+1236	CGCS 1124	
06129−0526 N	213.72	−10.49	5.52	0.53	0.44	06129−0525		
06179−0634 N	215.33	−9.89	6.15	0.83	0.38	06178−0634		
06198−0558 N	215.00	−9.20	4.82	0.82	0.36	06196−0558	CGCS 1249	
06256−1055 N	220.14	−10.12	5.75	0.69	0.26	06256−1055	CGCS 1283	
06271−1400 N	223.12	−11.14	5.34	0.85	0.37	06272−1400	CGCS 1289	
06465−2118 S	231.85	−10.13	4.55	0.69	0.36	06465−2118	CGCS 1416	
06505−2257 S	233.77	−10.01	5.40	1.10	0.33	06504−2258		
06553−2745 S	238.65	−11.10	5.98	0.78	0.44	06555−2744	CGCS 1490	
06574−1440 S	227.01	−4.87	4.38	1.02	0.27	06575−1441	CGCS 1502	
06589−1846 S	230.86	−6.40	6.07	0.46	0.44	06588−1847	CGCS 1513	
07001−2412 S	235.88	−8.59	6.62	0.79	0.21	07000−2411	CGCS 1517	
07018−1601 S	228.70	−4.54	4.47	0.78	0.39	07018−1601	CGCS 1532	
07027−1456 S	227.84	−3.85	4.38	2.53	0.42	07028−1456	CGCS 1540	
07030−1603 S	228.87	−4.30	5.09	1.43	0.37	07031−1604		see note a
07036−2221 S	234.57	−7.04	6.90	3.73	0.41	07036−2220		
07037−2326 S	235.56	−7.51	6.56	0.93	0.26	07039−2326		see note b
07055−1441 S	227.94	−3.14	5.86	1.01	0.29	07054−1442	CGCS 1562	
07060−1322 S	226.82	−2.42	5.24	0.71	0.34	07061−1323	CGCS 1567	
07091−2005 S	233.12	−4.88	6.15	0.75	0.40	07091−2004	CGCS 1591	
07099−2012 S	233.32	−4.76	4.03	2.89	0.42	07098−2012	CGCS 1601	
07100−1102 S	225.22	−0.46	5.41	1.05	0.36	07100−1101	CGCS 1602	
07104−1849 S	232.15	−4.00	6.18	0.93	0.29	07104−1849	CGCS 1606	
07114−1525 S	229.25	−2.23	4.65	0.85	0.32	07113−1526	CGCS 1611	
07116−1935 S	232.96	−4.13	3.32	0.88	0.32	07116−1936	CGCS 1612	
07118−1023 S	224.83	0.22	5.42	2.25	0.45	07118−1022	CGCS 6209	
07121−1155 S	226.23	−0.44	5.93	1.04	0.36	07120−1156		see note c
07124−1720 S	231.06	−2.90	3.66	0.74	0.35	07124−1720	CGCS 1615	
07127−1030 S	225.05	0.37	4.88	0.70	0.39	07129−1030	CGCS 1618	
07131−1728 S	231.25	−2.80	4.36	0.84	0.34	07132−1728	CGCS 1624	
07136−1513 S	229.32	−1.65	5.65	1.15	0.27	07136−1512	CGCS 1630	
07139−0907 S	223.96	1.28	5.87	1.10	0.24	07139−0907	CGCS 1631	
07141−1442 S	228.92	−1.31	5.47	0.88	0.28	07141−1442	CGCS 1632	
07145−1429 S	228.77	−1.11	4.53	1.90	0.32	07145−1428	CGCS 6214	
07163−1608 S	230.43	−1.53	4.85	0.62	0.45	07163−1608	CGCS 1648	
07189−0805 S	223.64	2.86	5.69	0.81	0.36	07189−0805	CGCS 1667	
07193−1529 S	230.20	−0.57	4.85	1.06	0.25	07194−1529	CGCS 1672	
07206−1032 S	225.99	2.05	4.16	0.99	0.30	07204−1032	CGCS 1682	
07208−1411 S	229.23	0.37	3.76	0.95	0.30	07208−1410	CGCS 1687	
07214−1525 S	230.39	−0.09	5.56	0.71	0.35	07215−1527	CGCS 1694	
07216−1245 S	228.06	1.22	4.19	2.90	0.37	07217−1246	CGCS 1696	
07222−1553 S	230.88	−0.16	5.31	1.12	0.15	07223−1553	CGCS 1701	
07225−0538 S	221.89	4.80	6.26	2.23	0.29	07227−0537	CGCS 6223	

Table 2—Continued

NIRS name	$l^{\text{II}}$	$b^{\text{II}}$	K	$K-L'$	$3.1 \mu\text{m}$	IRAS	CGCS	comments
07235–0354 S	220.49	5.84	3.64	0.98	0.28	07235–0356	CGCS 1708	J-type
07236–0505 S	221.54	5.31	4.75	0.75	0.42	07237–0505	CGCS 1709	
07245–1108 S	226.98	2.61	4.39	0.86	0.25	07245–1107	CGCS 1719	
07247–0901 S	225.15	3.67	4.48	1.85	0.31	07246–0903	CGCS 1720	
07250–0832 S	224.75	3.96	5.18	0.84	0.32	07249–0832	CGCS 1724	
07275–1152 S	227.97	2.91	5.38	0.88	0.31	07275–1152	CGCS 1733	
07288–1007 S	226.60	4.03	4.41	0.89	0.35	07288–1006	CGCS 1743	
07289–0823 S	225.08	4.89	5.12	0.78	0.34	07288–0824	CGCS 1742	
07298–0415 S	221.53	7.06	5.55	0.74	0.35	07299–0415	CGCS 1755	
07313–1149 S	228.38	3.74	6.31	0.61	0.45	07312–1148	CGCS 1767	Fig. 2
07336–1005 S	227.14	5.07	7.05	3.84	0.40	07336–1006	CGCS 6233	see note d
07486–0229 S	222.24	12.03	3.00	1.76	0.32	07487–0229	CGCS 1907	
11318–7256 N	297.33	–11.20	1.32	1.94	0.36	11318–7256	CGCS 3062	see note d
11372–7217 N	297.54	–10.45	2.01	0.51	0.39	11371–7216	CGCS 3083	
12545+6615 S	122.12	51.14	0.24	0.88	0.36	12544+6615	CGCS 3313	J-type
13411–7021 N	307.39	–8.21	2.62	0.98	0.28	13408–7021	CGCS 3425	
16010–5837 N	325.85	–4.80	3.57	0.44	0.36	16009–5837	CGCS 6615	
16522–4616 N	340.13	–1.91	3.61	1.07	0.34	16522–4616	CGCS 3745	
17055–4343 N	343.61	–2.19	3.41	1.25	0.30	17054–4342	CGCS 3773	
17131–3906 N	348.16	–0.60	4.45	2.51	0.39	17130–3907	CGCS 3794	
17145–3431 N	352.05	1.84	3.70	0.89	0.42	17146–3432	CGCS 3798	
17173–4019 N	347.64	–1.97	1.38	0.99	0.28	17172–4020	CGCS 3808	
17181–3812 N	349.47	–0.88	3.90	1.45	0.43	17183–3814		see note e
17233–3132 N	355.56	2.03	3.90	1.27	0.28	17233–3132	CGCS 3830	
17420–1836 N	8.74	5.48	2.23	0.62	0.44	17419–1838	CGCS 3875	
18306+3657 S	65.35	19.47	0.26	0.96	0.17	18306+3657	CGCS 4038	J-type
19028+2018 S	52.66	6.28	4.65	2.93	0.36	19029+2017	CGCS 6767	
19085+1329 S	47.21	1.94	4.54	0.98	0.44	19085+1327	CGCS 4192	
19109+1156 S	46.10	0.71	3.84	2.06	0.41	19108+1155	CGCS 4202	
19119+1022 S	44.83	–0.25	4.52	1.45	0.44	19118+1020		see note f
19121+1830 S	52.04	3.51	3.99	1.06	0.32	19122+1830	CGCS 4209	
19131+1718 S	51.11	2.73	3.60	0.97	0.30	19132+1719	CGCS 4211	
19155+0846 S	43.84	–1.80	3.71	1.09	0.30	19155+0847	CGCS 4224	
19181+1250 S	47.73	–0.44	4.03	0.99	0.34	19181+1249	CGCS 4238	
19188+0735 S	43.18	–3.06	4.95	0.93	0.36	19188+0733	CGCS 4240	
19207+1719 S	51.97	1.15	4.34	1.73	0.42	19207+1720	CGCS 4251	
19218+4607 N	77.99	14.12	5.07	0.65	0.40	19217+4607	CGCS 4260	
19225+1352 S	49.16	–0.88	4.99	0.76	0.36	19227+1354	CGCS 4261	
19248+0656 S	43.31	–4.67	3.48	2.43	0.43	19248+0658	CGCS 4275	Fig. 3
19284+1340 S	49.66	–2.23	4.55	1.02	0.28	19285+1340	CGCS 4312	
19353+0636 S	44.27	–7.15	3.25	0.87	0.26	19354+0636	CGCS 4373	
19505+5332 N	86.93	13.31	5.00	0.77	0.36	19505+5333	CGCS 4543	Fig. 5
20229–1641 S	27.84	–28.12	6.57	1.04	0.27		CGCS 4844	
20547+6404 N	100.56	12.21	4.70	2.31	0.41	20546+6405	CGCS 5053	
21263+6959 N	107.19	13.89	1.47	1.37	0.37	21262+7000	CGCS 5322	
21538+6916 N	108.51	11.74	5.03	0.74	0.39	21539+6916	CGCS 5507	

Table 2—Continued

NIRS name	$l^{\text{II}}$	$b^{\text{II}}$	K	$K-L'$	$3.1 \mu\text{m}$	IRAS	CGCS	comments
21563+7109 N	109.89	13.08	3.64	0.72	0.39	21560+7108	CGCS 5529	
05590+0637 N	201.27	−7.91	4.34	1.08	0.46	05591+0638	CGCS 1145	see note g
07175−0843 S	224.03	2.25	5.69	0.81	0.47	07175−0842	CGCS 1655	see note g
07289−0252 S	220.20	7.50	5.93	0.73	0.47	07290−0251	CGCS 1744	see note g
07281−1216 S	228.39	2.84	5.83	0.61	0.46	07280−1217	CGCS 1735	see note h

<sup>a</sup>A 30-min-exposure plate obtained by D.J. MacConnell shows nothing at this position. The R DSS2 plate has a faint star  $3''$  SE of the IRAS position

<sup>b</sup>A 30-min-exposure plate obtained by D.J. MacConnell shows a faint continuum (short and red) which has a general character of a carbon star but is too underexposed to be certain, although it has been tentatively identified as a C star by MacConnell (1979). The R DSS2 plate has a bright star at the IRAS position

<sup>c</sup>A 60-min-exposure plate obtained by D.J. MacConnell shows nothing at the IRAS position

<sup>d</sup>2.9–3.5  $\mu\text{m}$  spectrum also presented by Groenewegen et al. (1994)

<sup>e</sup>A 60-min-exposure plate obtained by D.J. MacConnell has a very red, non-C star east of the IRAS position which probably corresponds to the bright star  $32''$  away at position angle 66 deg. on the DDS2 I plate

<sup>f</sup>LRS spectrum C (11  $\mu\text{m}$  SiC emission, Kwok et al. 1997); tentative identification as a C star by Chen & Chen (2003)

<sup>g</sup>3.1  $\mu\text{m}$  index larger than 0.45 (paper II)

<sup>h</sup>3.1  $\mu\text{m}$  index larger than 0.45 (Tanaka et al., in preparation)